Electronic Supplementary Material (ESI) for Journal of Materials Chemistry A.

Supporting Information

Spray coating polymer substrates from a green solvent to enhance desalination performances of thin film composites

Shiliang Lin[a], Shanshan He[b], Sulaiman Sarwar[a], Roxana A. Milescu[c], Con R. McElroy[c]

, Simone Dimartino[a], Shao Lu[b], Cher Hon Lau* [a],

a. *School of Engineering University of Edinburgh Robert Stevenson Road, EH9 3FK, United Kingdom E-mail: cherhon.lau@ed.ac.uk*

b. *MIIT Key Laboratory of Critical Materials Technology for New Energy Conversion and Storage, State Key Laboratory of Urban Water Resource and Environment, School of Chemistry and Chemical Engineering, Harbin Institute of Technology, Harbin 150001, PR China*

c. *Department of Chemistry, Green Chemistry Centre of Excellence, University of York, Heslington, York YO10 5DD, United Kingdom*

1. 3D printer modification

Figure S1 shows modifications of a 3D printer to enable automated spray coating. Fig S1a shows the original state of a FlashForge CreatorPro 3D printer. On top of the moving tray, there is a dual-printhead installed. Tray movement is generated from the the x-axis and y-axis stepper motor. To modify this 3D printer into an automated spray coater, we designed a housing for the spray gun and a servo motor that controls the spray gun (Fig S1b). Servo motor motion is used here to control the nozzle gap of the spray gun. After installing the entire housing on top of the moving tray and connected to pressurized Nitrogen supply (Fig S1c), we then designed a programable control circuit using one Arduino Nano and two A4988 stepper motor control boards. The Arduino board generates PWM signals and sends these

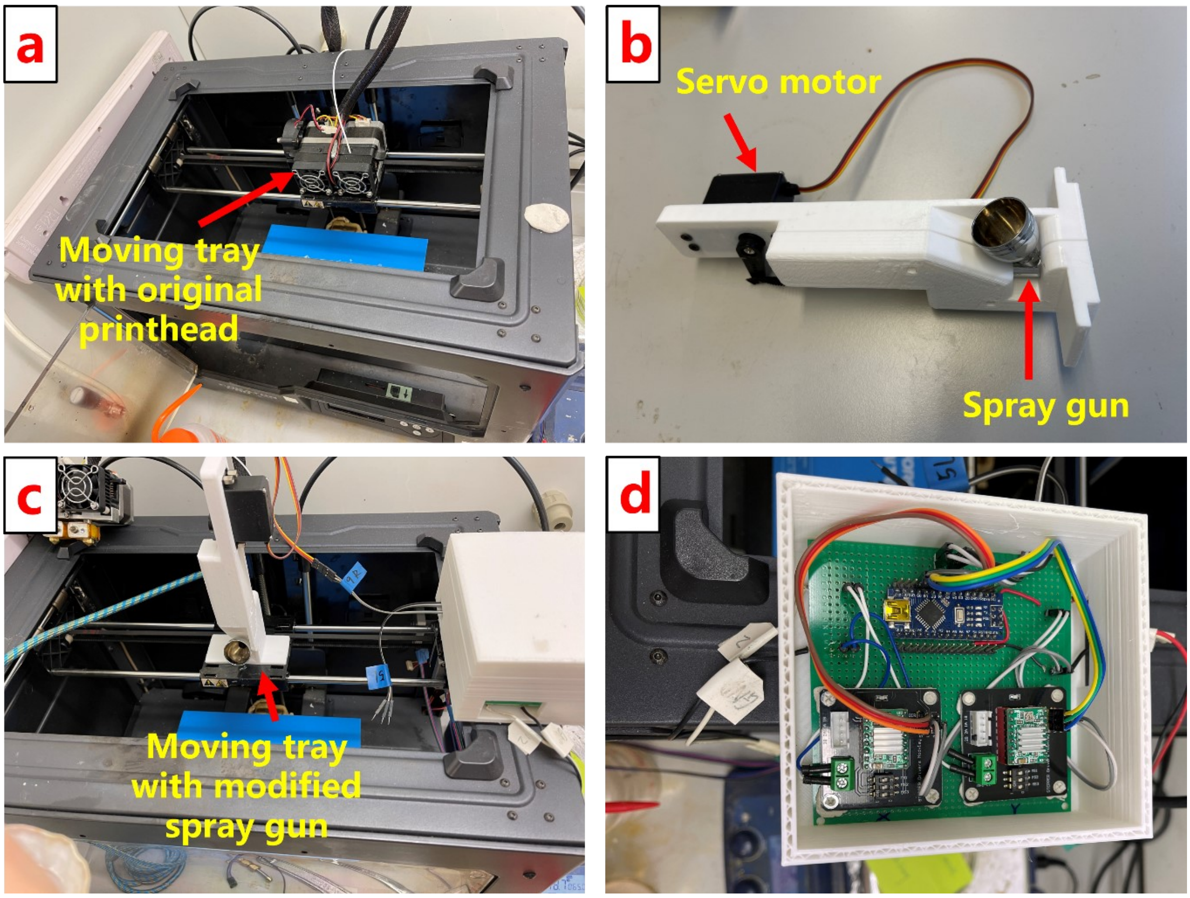

signals to the stepper motor control board to generate the movement.

Figure S1. Modification of the 3D printer. a) Original 3D printer with its dual-printhead, b) CRplus Action Airbrush installed inside a housing with a servo motor, c) the original printhead was removed and spray gun was installed onto the moving tray, d) Control circuit with an Arduino Nano and two A4988 stepper motor control boards.

2. Spray coating method membrane building process

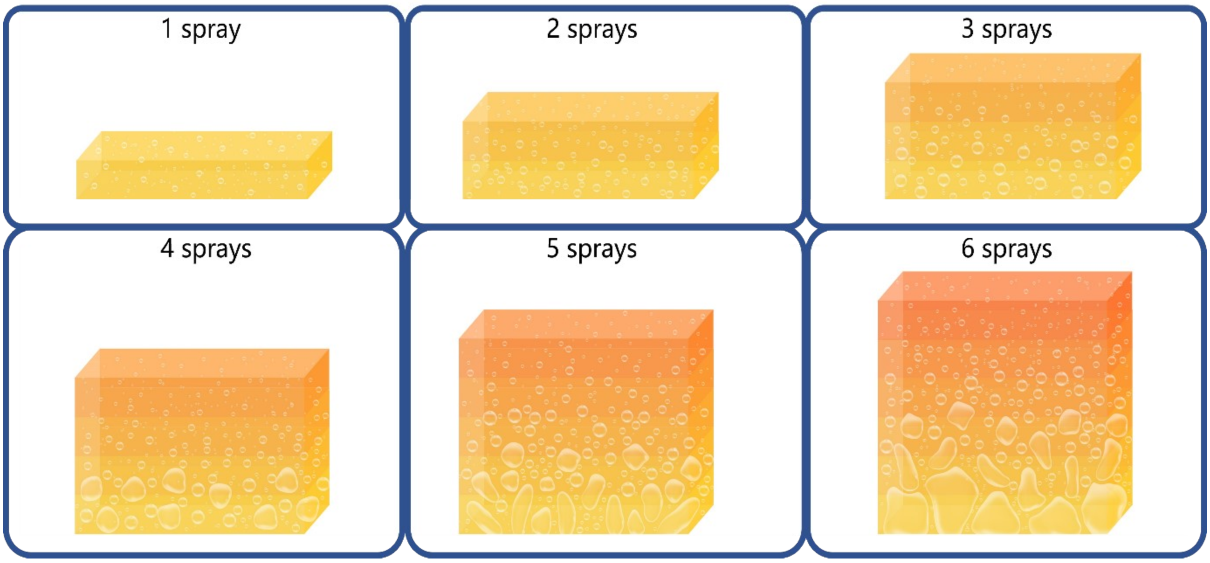

Figure S2. Illustration of spray coating process to build up polymer layers during membrane fabrication. A 200 um thick PES membrane is formed after 6 times of spray coating.

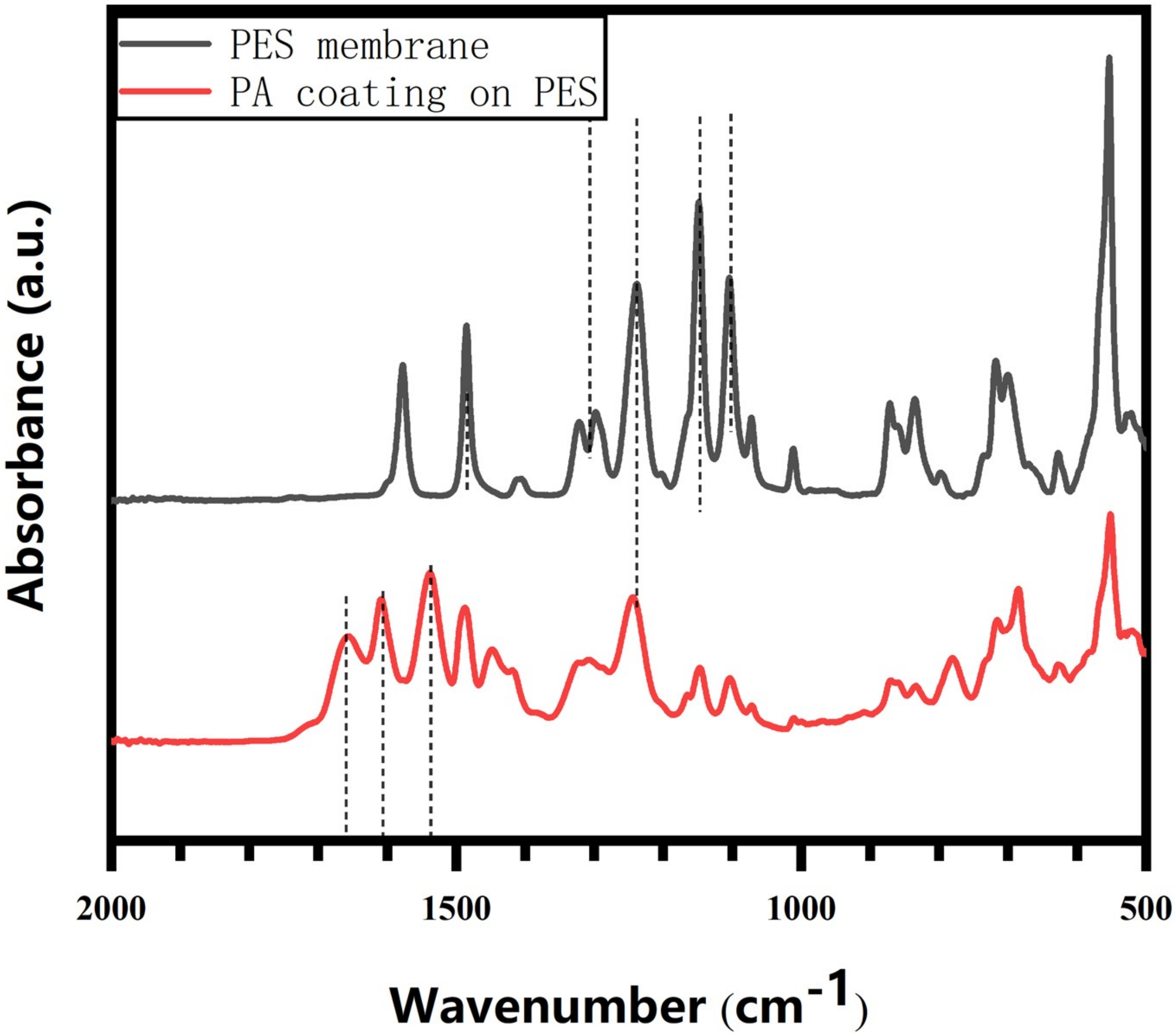

3. ATR-FTIR of spray coated PES supports and PA/PES TFC membrane.

Figure S3. ATR-FTIR absorption spectra of PES membrane fabricated by spray coating and PA selective layer deposited on this PES membrane.

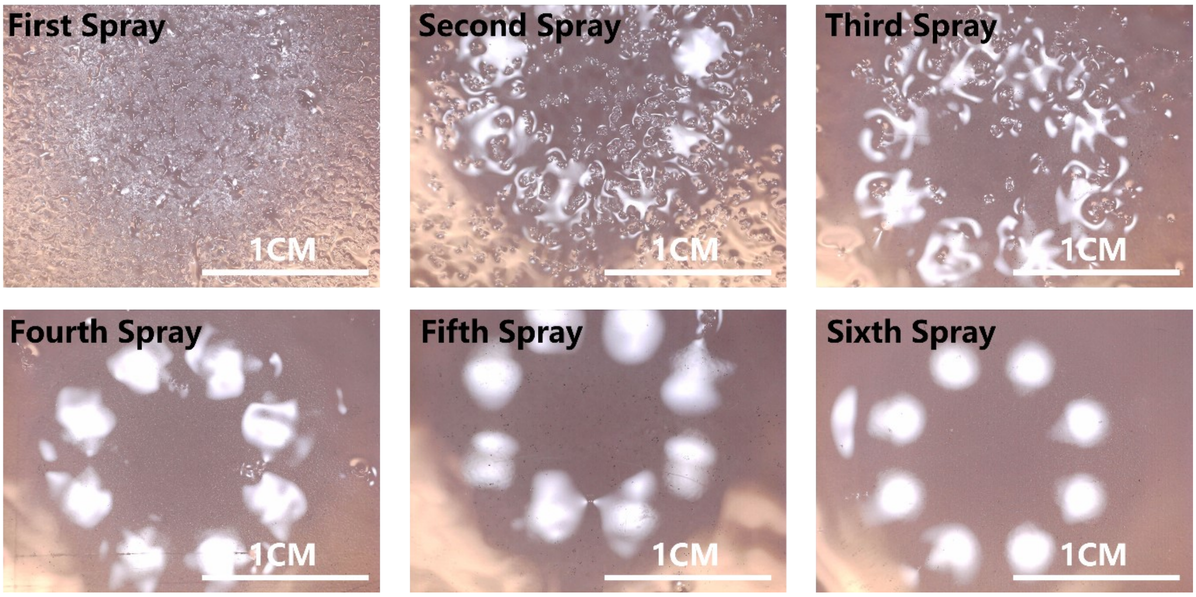

4. Spray coating method membrane building process

Figure S4. Optical microscopy images showing the layer-by-layer build-up of C-PES-S-1 dope solution. Gaps between partially connected islands of dope solution in first layer were subsequently filled up as spray coating was repeated for 6 times.

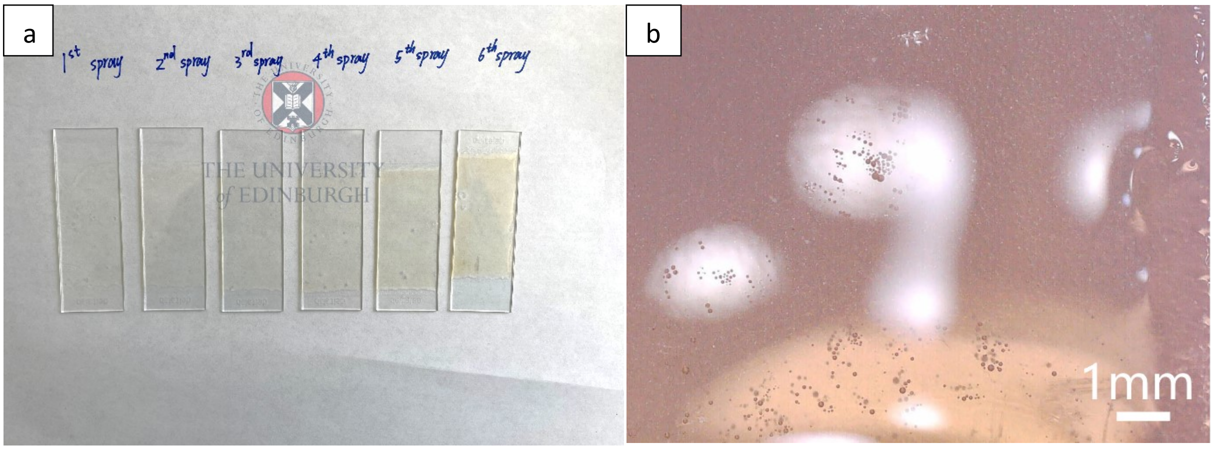

Figure S5. a) Spray coating C-PES-S-1 Dope solution on top of a glass plate with different spray coating repetitions; b) Enlarged image of dope film after 6 times of spray coating showing 0.1 to 0.15 μm large air bubbles .

5. Scanning electron microscopy (SEM) of PES membranes

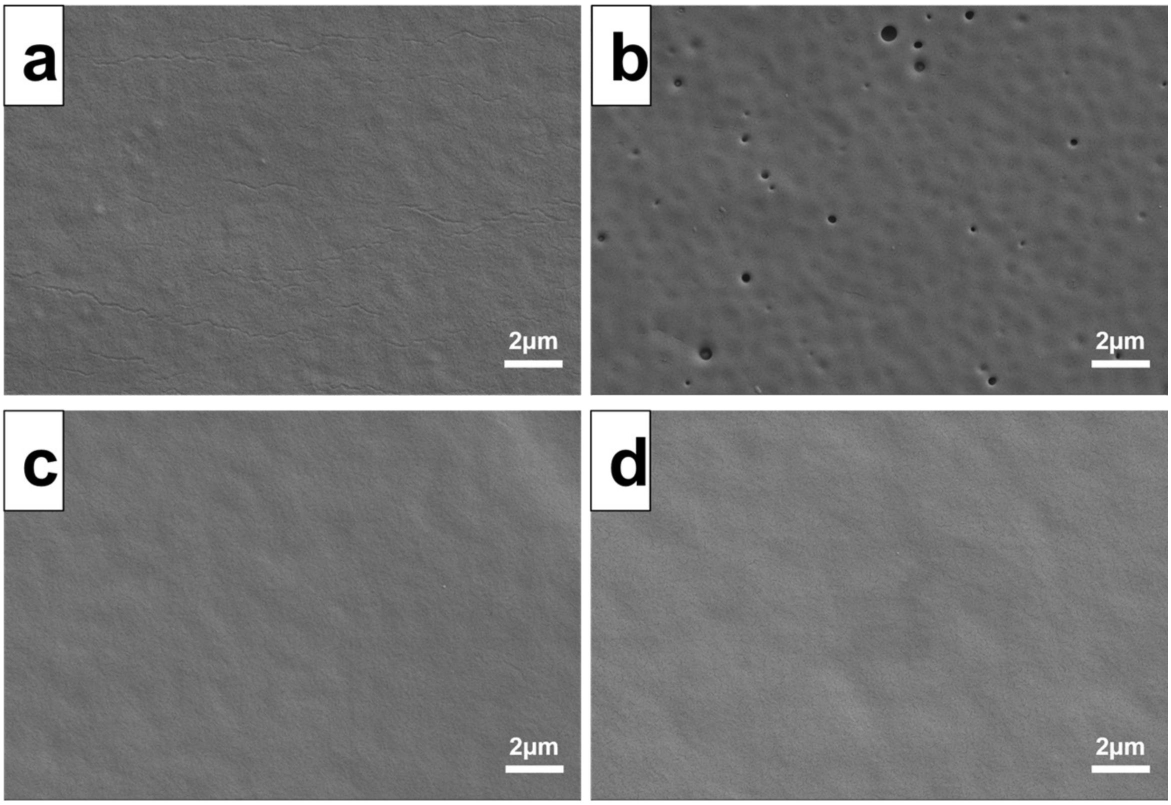

Figure S6. SEM micrographs showing surface morphology of N-PES-C samples, with a) 0 wt.%, b) 1 wt.%, c) 3 wt.% and d) 5 wt.% PVP loading.

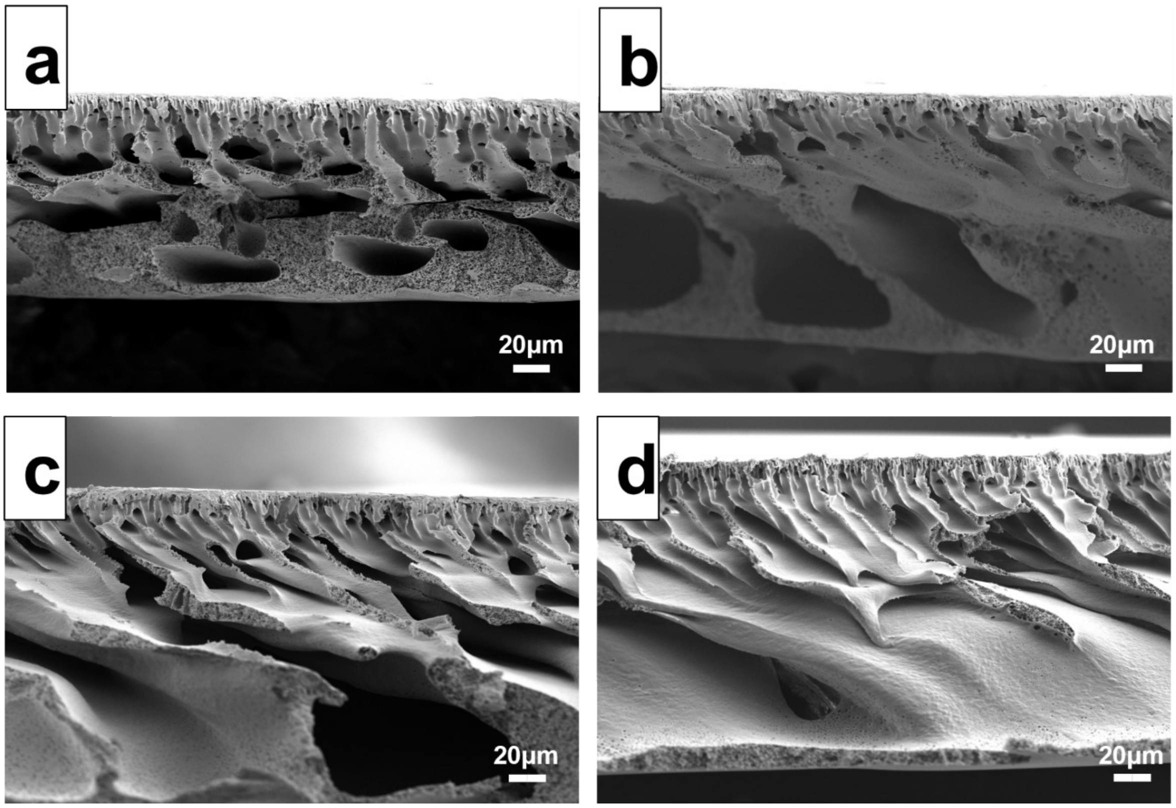

Figure S7. SEM micrographs showing the cross-sections of N-PES-C samples with different PVP loading. a) 0 wt.%, b) 1 wt.%, c) 3 wt.% and d) 5 wt.%.

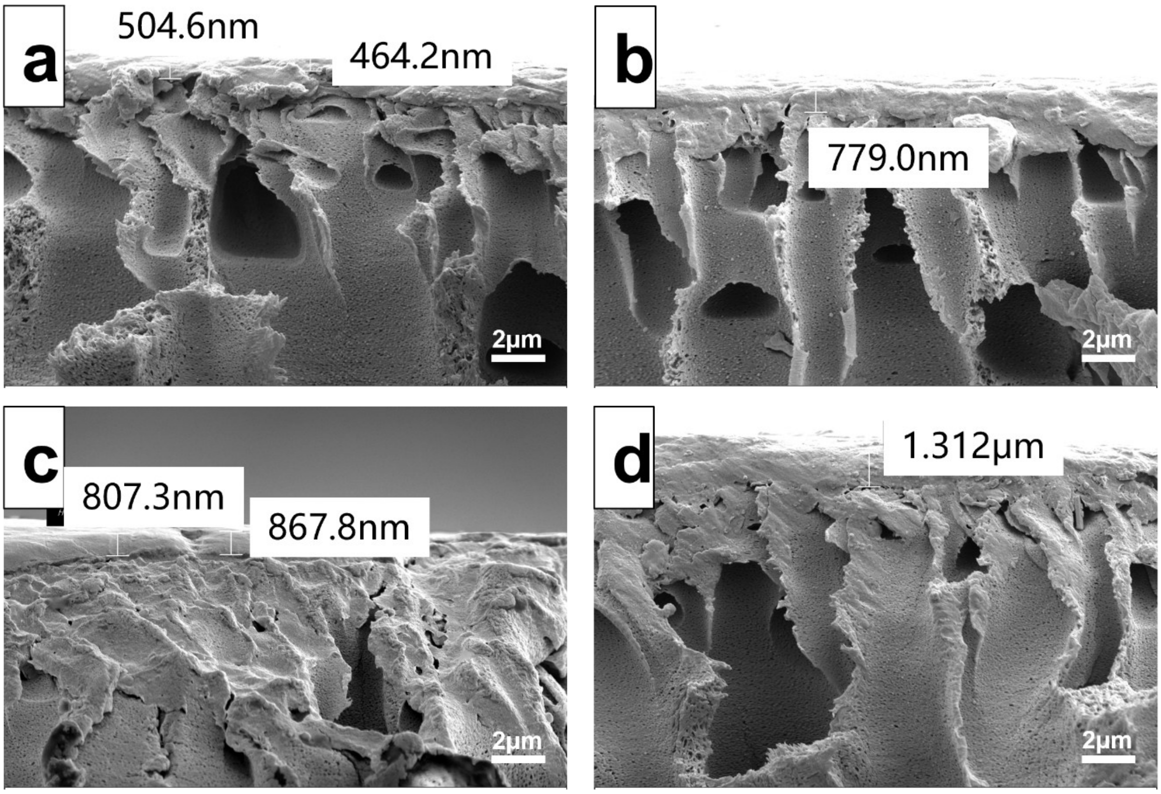

Figure S8. SEM micrographs showing the skin layer thickness of the N-PES-C membrane with a) 0 wt.%, b) 1 wt.%, c) 3 wt.% and d) 5 wt. % PVP loading.

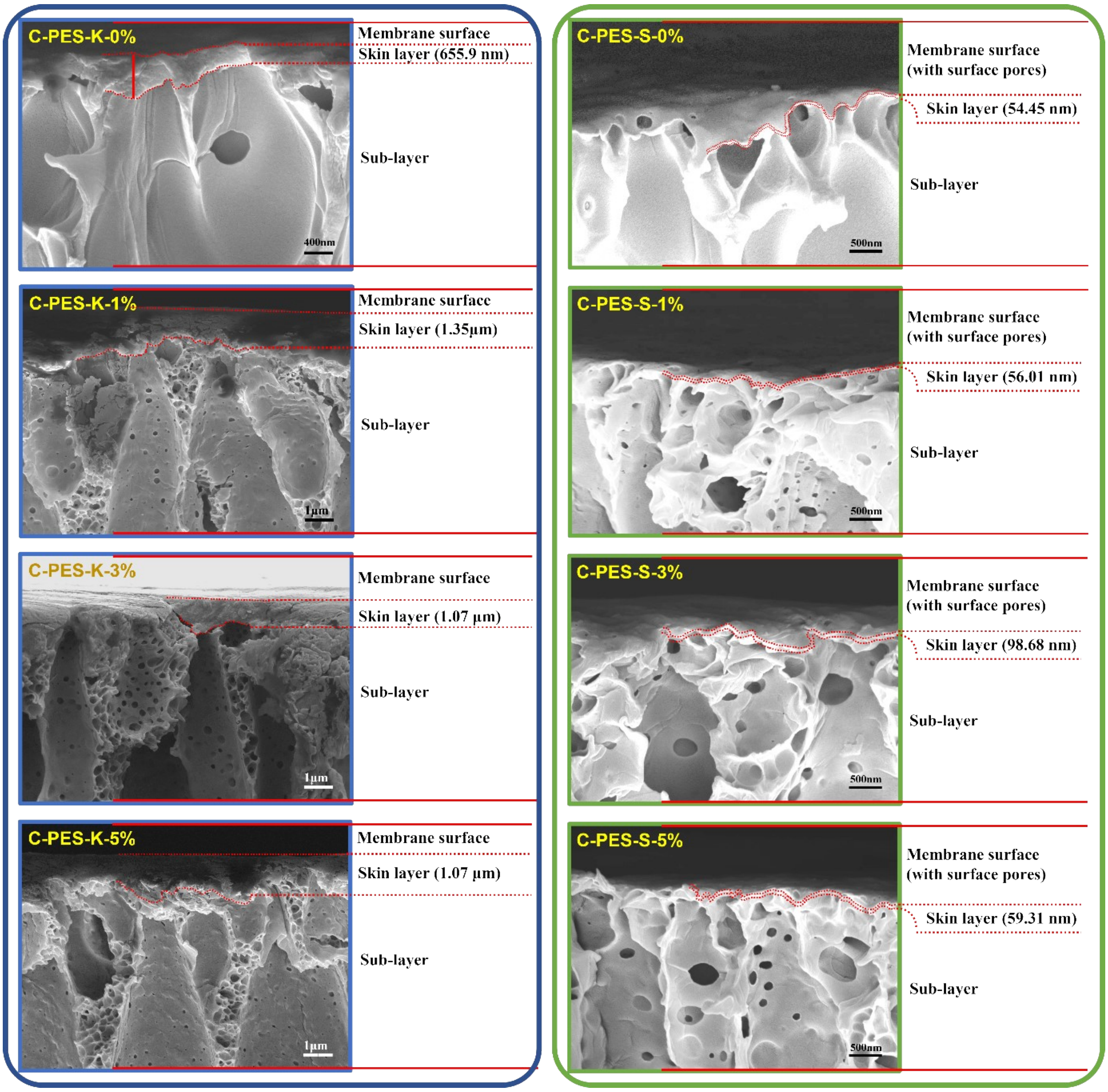

Figure S9. SEM micrographs comparing the skin layer thicknesses of knife-cast (outlined in blue boxes) and spray coated (outlined in green boxes) PES membranes fabricated using Cyrene-based dope solutions with various PVP loadings.

6. Membrane stability

A. Cyclic water filtration measurements

To observe the effect of pressure on membrane fluxes, the pure water fluxes of these samples were measured at 3 bar and repeated 5 times. The pure water fluxes of these membranes were consistent, indicating that these membranes were mechanically stable at 3 bar.

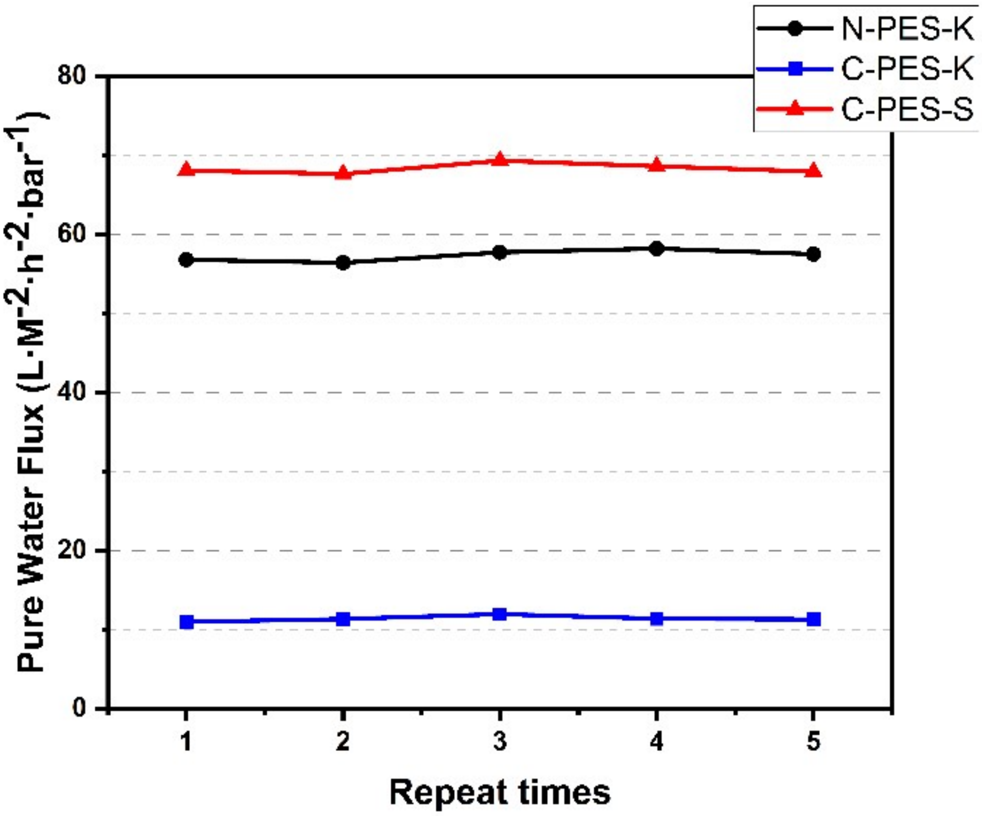

Figure S10. Cyclic water filtration tests of PES membranes fabricated *using* different methods (knife-casting) and solvents (NMP, Cyrene). All membranes were tested under 3 bar and 1 hour for each cycle.

B. Tensile stress

Stress is defined as the force (N) per unit area (m^2), normal to the direction of the applied force. The tensile stress of these membranes were measured using a universal testing machine (Instron 4500 model) at a crosshead speed of 2 mm/min. Cross sectional area of the sample of known width and thickness was calculated. The membranes were then placed between the grips of the testing machine. The tensile stress values and elongation at break values of the individual membranes were measured and are shown in Table S1.

Table S1. Tensile stress of PES membranes fabricated via different methods and solvents

	C-PES-K-1%	C-PES-S-1%	N-PES-K-1%
Tensile stress (MPa)	2.619	2.096	2.208

Amongst all PES membranes studied here, the tensile stress of membranes produced from knife-casting Cyrene-based dope solutions were the highest, reaching 2.62 MPa, followed by N-PES-K and C-PES-S samples. This could be attributed to the order of skin layer thickness[1]. For SEM cross-section images, we observed that the skin layer of C-PES-K membranes were thickest, reaching 1.071μm (Fig. S9). Meanwhile the skin layer thicknesses of N-PES-K and C-PES-S samples were 779.0nm and 56.01nm. For the N-PES-K-1% and C-PES-S-1% sample, with similar overall thickness but higher content and bigger size of macrovoid in the sub-layer[2], C-PES-S-1% should have a lower tensile stress at break.

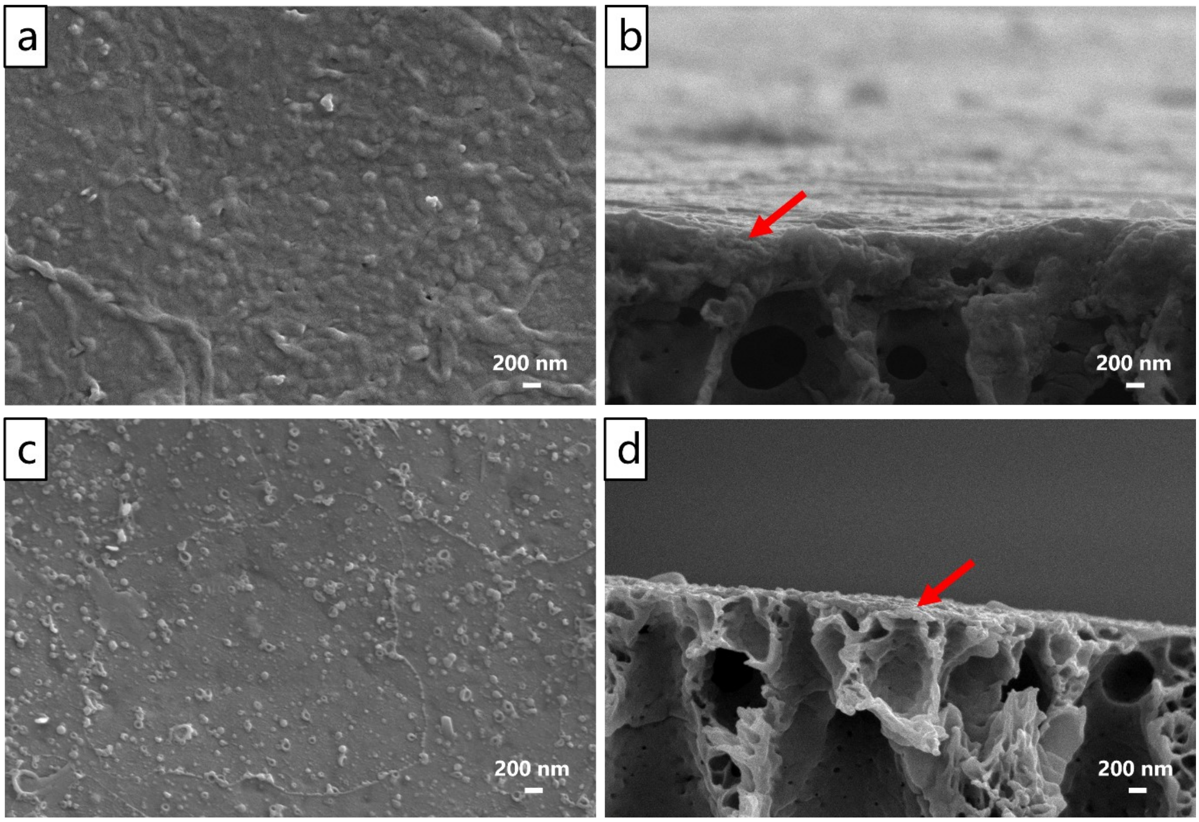

7. Scanning electron microscopy (SEM) of PES membranes

Figure S11. SEM micrographs showing PA layer deposited on top of different PES supports, a) surface of PA/C-PES-K-1; b) Cross-section image of PA/C-PES-K-1; c) surface of PA/C-PES-S-1; cross-section image of PA/C-PES-S-1.

References

1. G. Arthanareeswaran and V. M. Starov, *Desalination*, 2011, **267**, 57-63.
2. S. A. Al Malek, M. N. Abu Seman, D. Johnson and N. Hilal, *Desalination*, 2012, **288**, 31-39.